February, 1993] *Bull. Chem. Soc. Jpn.*, ***66***, *541—549(1993)*

Reductive Photoallylation of Dimethyl Naphthalenedicarboxylates by Allyltrimethylsilane via a Single Electron Transfer

Yasuo KUBO,* Toshiko TODANI, Takeo INOUE, Hisanori ANDO, and Takaji FUJIWARA
Department of Chemistry, Faculty of Science, Shimane University, Matsue, Shimane 690

(Received August 17, 1992)

The photoreaction of dimethyl 1,4-naphthalenedicarboxylate (**4**) with allyltrimethylsilane (**7**) in acetonitrile–methanol gave reductive allylation products. The formation of the products is rationalized by a mechanism involving a single electron transfer from **7** to the singlet excited state of **4**, an attack of the allyl radical (**16**) generated by a C–Si bond cleavage in the radical cation of **7** toward the radical anion of **4** to give an anionic intermediate, and protonation of the intermediate. The photoreaction of dimethyl 1,2-naphthalenedicarboxylate (**2**) with **7** gave reductive allylation products along with a cyclobutane, possibly by the secondary photoreaction of another reductive allylation product. The photoreactions of dimethyl 1,3-, 2,3-, and 2,6-naphthalenedicarboxylates (**3**, **5**, and **6**) with **7** gave cyclobutanes, possibly by the photoreactions of reductive allylation products. The values of the free-energy changes (ΔG_{et}) associated with the single-electron transfer from **7** to the singlet excited states of **2**—**6** and the fluorescence quenching rate constant (k_{q}) support the photochemical single-electron transfer mechanism. The attacking position of **16** toward the radical anions of **2**—**6** and the position of the protonation of anions resulting from an attack of **16** are discussed on the basis of the values of the spin densities of the radical anions of **2**—**6** obtained by MNDO calculations and the net atomic charges of the model anions.

The area of single-electron transfer photochemistry has received much attention regarding both synthetic and mechanistic aspects in organic photochemistry.[1] The single-electron transfer in neutral excited donor-acceptor pairs normally leads to the generation of radical ion intermediates, which can undergo rapid reactions to produce secondary radicals or charged intermediates in routes for product formation. In order to find ways for synthetic applications of the single-electron transfer photoreactions it is, thus, important to understand the factors which affect the chemical course from the radical ion intermediates as well as those which affect the single-electron transfer process, itself. Although aromatic nitriles have been used as typical neutral electron acceptors in a large portion of the investigations carried out so far, the radical anions of the aromatic nitriles have sometimes caused complex secondary reactions, mainly due to the elimination pathways opened for the CN-group, making the analysis and prediction of the chemical course after a single-electron transfer complicated. We started our investigation concerning the single-electron transfer photoreactions of aromatic esters, since an elimination of the ester-group from the radical anions seems to be unlikely, and the reaction pathways from the radical anions are expected to become simpler, compared with those from the radical anions of the aromatic nitriles. Little information has been reported concerning the single-electron transfer photoreactions of aromatic esters.[2]

In this study one aromatic monoester, methyl 2-naphthalenecarboxylate (**1**), and five aromatic diesters, dimethyl 1,2-, 1,3-, 1,4-, 2,3-, and 2,6-naphthalenedicarboxylates (**2**—**6**), were used as acceptors. Allyltrimethylsilane (**7**) was chosen as a typical donor, since reductive allylations via a single-electron transfer from **7** to excited iminium cations,[3] cyano compounds,[4] and aromatic imides[5] had already been reported. Reductive photoallylations of the diesters **2**—**6** by **7** were found to proceed in acetonitrile–methanol, although no photoreactions of the monoester **1** with **7** were observed. The reductive photoallylations of **2**—**6** by **7** gave simpler products, compared with those of the corresponding aromatic cyanide, as shown in Eq. 1;[4b] thus, the chemical course after the single electron transfer could be easily analyzed.

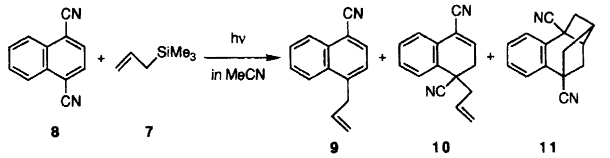

(1)

Results and Discussion

Fluorescence Quenching and Calculations of the Free Energy Change ΔG_{et} Associated with Single Electron Transfer. Esters **1**—**6** show clear fluorescence in air-saturated acetonitrile with the lifetimes (τ) given in Table 1. The fluorescence of diesters **2**—**6** was quenched by **7** to various extents without changing the shape or wavelength of the maximum emission. Stern–Volmer plots of the fluorescence quenching by **7** in air-saturated acetonitrile gave straight lines against the concentration of **7**. The fluorescence quenching rate constants (k_{q}) calculated from the Stern–Volmer slopes ($k_{\mathrm{q}}\tau$) and the τ values are also shown in Table 1. The fluorescence of the monoester **1** was hardly quenched by **7**.

The free-energy changes (ΔG_{et}) associated with a single-electron transfer from **7** to the singlet excited states

Table 1. Quenching of the Fluorescence of Methyl 2-Naphthalenecarboxylate (**1**) and Dimethyl Naphthalenedicarboxylates **2**—**6** by Allyltrimethylsilane (**7**) in Acetonitrile[a)]

Position of ester group	Compd	$k_q\tau^{b)}/\mathrm{M}^{-1}$	τ/ns	$k_q/\mathrm{M}^{-1}\,\mathrm{s}^{-1}$
2	**1**	$0^{c)}$	7.5	$0^{c)}$
1,2	**2**	5.9	6.8	8.7×10^{8}
1,3	**3**	23	6.2	3.7×10^{9}
1,4	**4**	32	8.5	3.8×10^{9}
2,3	**5**	0.15	6.3	2.4×10^{7}
2,6	**6**	3.3	9.4	3.5×10^{8}

a) Experimental conditions are as follows; [**1**—**6**]= 1×10^{-4} M, at 25°C, in an air-saturated acetonitrile. b) Stern–Volmer slope for the fluorescence quenching. c) No fluorescence quenching was observed.

of **1**—**6** can be calculated by using[6)]

$$\Delta G_{\mathrm{et}} = 23.06[E(\mathrm{D/D^+}) - E(\mathrm{A^-/A})] - E_{\mathrm{S}} - \mathrm{C}. \qquad (2)$$

In this equation $E(\mathrm{D/D^+})$ is the one-electron oxidation potential for **7** (1.94 V),[3a)] $E(\mathrm{A^-/A})$ is the one-electron reduction potential for **1**—**6** (in Volts), E_{S} is the energy of the singlet excited state of **1**—**6** (in kcal mol^{-1}, 1 cal=4.184 J), and C is the "Coulombic attraction term" (1.3 kcal mol^{-1}) in acetonitrile.[6)] The $E(\mathrm{A^-/A})$ values determined by cyclic voltammetry, the E_{S} values estimated from the absorption and fluorescence spectra, and the calculated ΔG_{et} values are summarized in Table 2.

The k_q values given in Table 1 correlate well with the ΔG_{et} values in Table 2; i.e., the k_q value increases with decreasing ΔG_{et}. Judging from the k_q and ΔG_{et} values, the single-electron transfer from **7** to the singlet excited states of esters **1**—**6** can be expected to occur in the order **3**≅**4**>**2**≅**6**>**5**≫**1**. The photochemical single-electron transfer process to diesters **2**—**4** and **6** appears to be possible, though the process to diester **5** may be slow and the process to monoester **1** impossible.

Photoreactions of the Esters 1—6 with 7. No photoreactions of monoester **1** with **7** were observed, although photoreactions of diesters **2**—**6** with **7** proceeded, as mentioned below. The large positive ΔG_{et} value (3.3 kcal mol^{-1}) and the negligibly small k_q value can account for the reactivity of **1** toward **7**.

Table 2. Calculated Free-Energy Changes (ΔG_{et}) Associated with Single-Electron Transfer from Allyltrimethylsilane (**7**) to the Singlet Excited States of Methyl 2-Naphthalenecarboxylate (**1**) and Dimethyl Naphthalenedicarboxylates **2**—**6**

Position of ester group	Compd	$E(\mathrm{A^-/A})^{a)}$ V	E_{S} kcal mol^{-1}	$\Delta G_{\mathrm{et}}{}^{b)}$ kcal mol^{-1}
2	**1**	−1.92	84.4	3.3
1,2	**2**	−1.64	83.4	−2.1
1,3	**3**	−1.57	84.4	−4.8
1,4	**4**	−1.35	80.0	−5.4
2,3	**5**	−1.79	84.1	0.6
2,6	**6**	−1.55	81.0	−1.8

a) Experimental conditions for the measurements are as follows; [**1**—**6**]=1×10^{-3} M in 0.1 M $\mathrm{Bu_4NClO_4}$/acetonitrile, at ambient temperature, with a platinum electrode vs. Ag/0.01 M $\mathrm{AgClO_4}$. b) Calculated by Eq. 2.

The photoreaction (>320 nm) of 1,4-diester **4** (2 mM, 1 M=1 mol dm^{-3}) with **7** (126 mM) in acetonitrile–10% methanol under $\mathrm{N_2}$ gave reductive allylation products **12** (51%) and **13** (22%), as shown in Eq. 3.

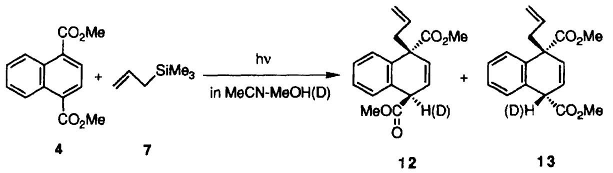

(3)

The structures of **12** and **13** were determined by their spectroscopic properties. The stereochemistry of **12** and **13** was confirmed mainly by the shielding effect in the chemical shift of the methine proton $\mathrm{CH_2{=}C\underline{H}CH_2}$– of **13**. Thus, the signals (δ=5.38) of **13** show a high-field shift relative to the corresponding methine signals (δ=5.63) of **12**. Molecular model examinations show that the allyl group of **13** can more freely rotate above the aromatic ring, compared with that of **12**, in which one of the methoxycarbonyl groups with a cis-arrangement, referred to as the allyl group, prevents any rotation of the allyl group.

The isomer ratio **12**/**13** remained almost constant during the course of the photoreaction. Products **12** and **13** were photostable under the irradiation conditions. The photoreaction of **4** with **7** in acetonitrile–10% $\mathrm{CH_3OD}$ led to **12** and **13** with a single deuterium, as shown in Eq. 3. The D contents in **12** and **13** were 87 and 83%, respectively. The D contents were maintained almost constant during the course of the photoreaction.

The formation of **12** and **13** is rationalized by a mechanism involving an initial single-electron transfer from **7** to the singlet excited state of **4** to give a pair of radical anions (**14**) of **4** and a radical cation (**15**) of **7**, as shown in Eq. 4.

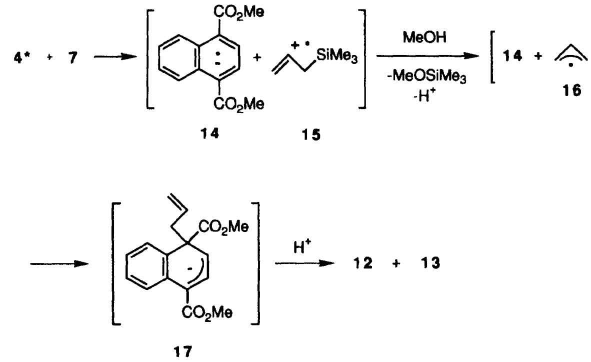

(4)

An attack of the allyl radical (**16**) generated by C–Si bond cleavage in **15** toward **14** affords the anionic intermediate **17** which gives **12** and **13** upon protonation. The deuterium incorporation observed in a reaction in the presence of CH_3OD is consistent with the final protonation process. The results of photoreaction indicate that the attack of **16** toward **14** occurs only at the 1-position of the naphthalene ring of **14**, and that protonation to **17** proceeds only at the α-carbon atom of the methoxycarbonyl group.

It should be emphasized here that the photoreaction of **4** with **7** was simpler and gave different types of products, compared with that of 1,4-dicyanonaphthalene (**8**) with **7**, as shown in Eq. 1.[4b)] The mechanism of the reaction of **8** with **7** and that of **4** with **7** appear to resemble each other, and the observed attacking positions of the allyl group are common. The difference in the type of observed products is, thus, accounted for by the different chemical course from the anion intermediates derived from an attack of **16** to the radical anions of **7** and **8**: The CN-group can easily leave from an anion intermediate, such as cyanide, but the methoxycarbonyl group cannot. The position of the hydrogen atom introduced in **10** is also different from those in **12** and **13**.

Upon a treatment with potassium hydroxide in ethanol, **12** gave a more stable isomer **18**, in which the double bond conjugated to the aromatic ring and the methoxycarbonyl group (Eq. 5).

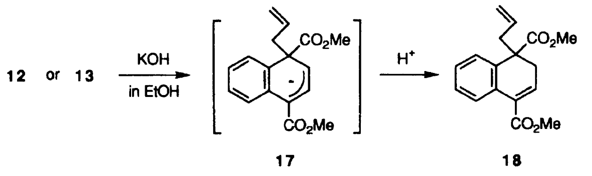

(5)

The same product **18** was obtained starting from **13**. Isomerization may occur through an anionic intermediate **17**, which already appeared as a precursor of **12** and **13** in Eq. 4. Thus, under kinetically controlled conditions, the protonation of **17** may give **12** and **13**; and under thermodynamically controlled conditions it affords **18**.

When **18** was irradiated in acetonitrile a cyclobutane **19** was formed by intramolecular [$2\pi+2\pi$] cycloaddition in almost quantitative yield (Eq. 6).

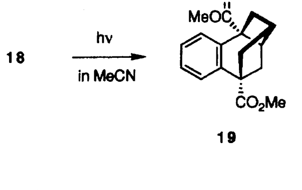

(6)

The structure of **19** is strongly supported by the ^{1}H NMR coupling constants, compared with those calculated using the parameters reported by Williamson and Johnson,[7)] on the basis of the dihedral angles obtained from an optimized structure determined by MM2 calculations for the mother compound, as shown in Table 3. No isomeric structures of **19** can rationalize the observed coupling constants.

The photoreaction of 1,2-diester **2** (2 mM) with **7** (126 mM) in acetonitrile–10% methanol gave reductive allylation products **22** (43%) and **23** (15%) together with a cyclobutane **25** (20%), as shown in Scheme 1. The stereochemistry of **22** and **23** was also confirmed by the shielding effect in the chemical shift of the methine proton $CH_2=C\underline{H}CH_2-$ of **23**. Thus, the signals ($\delta=5.65$) of **23** show a high-field shift relative to the corresponding methine signals ($\delta=5.90$) of **22**. The structure of **25** is also supported by the ^{1}H NMR coupling constants, as shown in Table 3. The formation of **25** is rationalized by the secondary photoreaction of the precursor **24**, which arises from **21** by protonation (Scheme 1). Attempts to isolate **24** were unsuccessful, possibly due to the photolability of **24**. No isomeric cyclobutanes of **25** could be observed in the reaction mixture. Thus, in the photoreaction of **2** with **7** an attack of **16** occurs both at the 1- and 4-positions of the naphthalene ring of the radical anion of **4**; an attack at the 4-position to give **22** and **23** predominates over that at the 1-position to give **25**. On the other hand, the protonation of **20** and **21** proceeds only at the α-carbon atoms of the methoxycarbonyl groups.

The photoreactions of 1,3-, 2,3-, and 2,6-diesters **3**, **5**, and **6** (each 2 mM) with **7** (126 mM) in acetonitrile–10% methanol gave cyclobutanes **28** (46%), **31** (31%), and **34** (55%), as shown in Eqs. 7, 8, and 9, respectively.

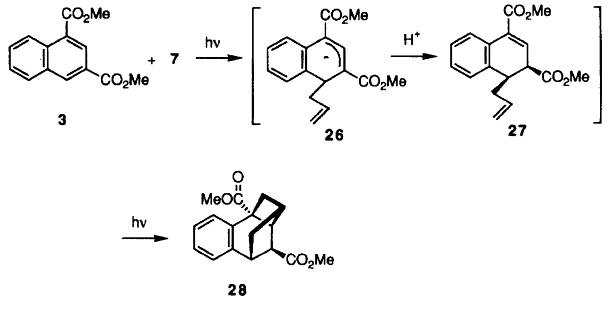

(7)

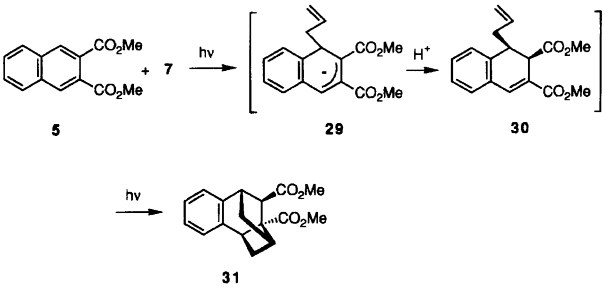

(8)

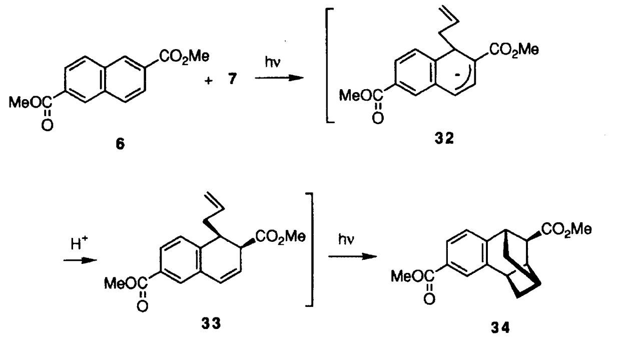

(9)

The structures of **28**, **31**, and **34** are also supported by the ^{1}H NMR coupling constants, as shown in Table 3. The formation of **28**, **31**, and **34** is rationalized by the secondary photoreactions of precursors **27**, **30**, and **33**, which arise from **26**, **29**, and **32** by protonation, respectively. Attempts to isolate **27**, **30**, and **33** were also unsuccessful. Thus, in the photoreactions of **3**, **5**, and **6** with **7** an attack of **16** occurs at the 4-, 1-, and 1-positions of the naphthalene ring of the radical anions of **3**, **5**, and **6**, respectively. The photoreaction of 2,3-diester **5** with **7** was considerably slow compared with those of the other diesters **2**—**4** and **6**, possibly reflecting the small positive ΔG_{et} value (0.6 kcal mol^{-1}).

In summary, the essential photoreactions of diesters **2**—**6** with **7** are reductive allylations, an attack of **16** toward the radical anions of the diesters followed by protonation. If the reductive allylation product has a double bond conjugated with the aromatic ring, the double bond will be able to absorb light, and efficient intramolecular cycloaddition will take place to give a cyclobutane. If the reductive allylation product has a double bond that is not conjugated with the aromatic ring, the product will be stable. Interesting features of the reductive allylations are that the position, at which the attack of **16** occurs, depends largely on the structures of the diesters, in other words, on the positions of the two methoxycarbonyl groups on the naphthalene ring; the position of the protonation also depends on the structures of the anions arising from an attack of **16** toward the radical anions of the diesters. In the next sections the factors which determine the attacking position of **16** and the position of the protonation are discussed.

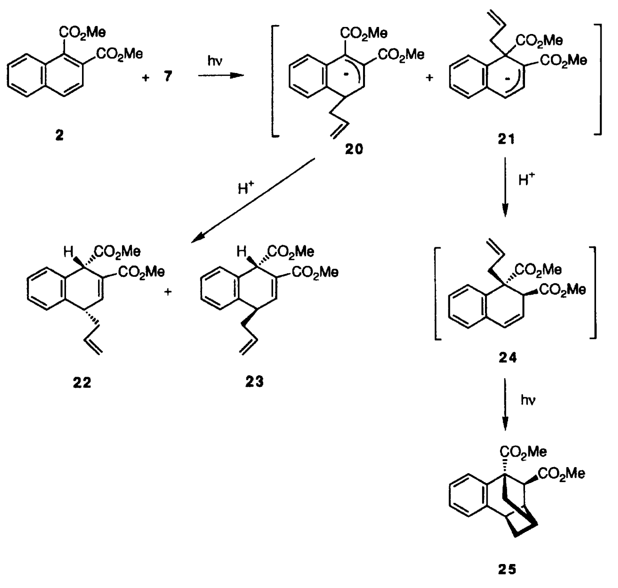

Scheme 1.

Factors Determining Attacking Positions of Allyl Radical (16). The observed attacking positions of **16** are simply shown in Chart 1 by arrows on the structural formulas of **2**—**6**. The key step which determines the attacking position is the coupling process between the radical anions of **2**—**6** and **16** on the basis of the mechanistic scheme shown in Eq. 4. Thus, the spin density on the respective atoms of the radical anions of diester **2**—**6** can play a primarily important role in determining the attacking position. Correlations between the product distributions and the spin densities of the radical ions have already been pointed out in reactions via coupling between the radical ions and radicals.[8] We therefore carried out MNDO RHF calculations[9] on the spin densities of the radical anions of **2**—**6** with geometry optimization; the results are given in Table 4. The results show that the positions indicated by the arrows on the structural formulas of diesters **3**, **4**, and **5** in Chart 1 correspond well with those at which the highest spin densities of the radical anions of diesters **3**, **4**, and **5** are observed (Table 4), and thus support the important role of the spin density of the radical anions in determining the attacking positions.

However, some conflicts between the observed attacking positions and the predicted positions from spin-density consideration are observed for diesters **2** and **6**. Thus, an attack of **16** at the 4-position (spin density; 0.1768) predominates over that at the 1-position (spin density; 0.2568) for **2**, and an attack occurs only at the 1-position (spin density; 0.1121) for **6**, in spite of the higher spin density (0.1644) at the 2-position. In these cases, differences between the spin densities of the two positions are not very large, and the steric effect due to the methoxycarbonyl groups at the 1- and 2-positions of **2** and **6**, respectively, may account for the conflicts

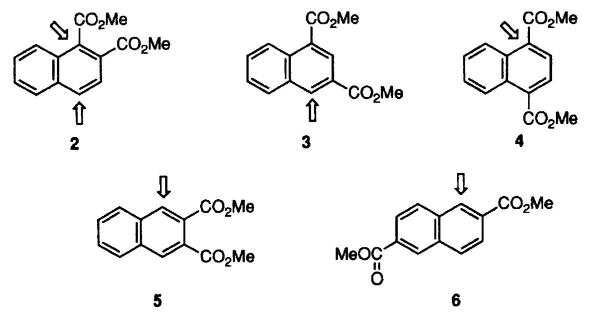

Chart 1.

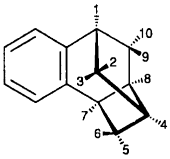

Table 3. ^{1}H NMR Spectral Data for Dimethyl 1,2,2a,3,4,8b-Hexahydro-2,4-methanocyclobuta[*a*]naphthalenedicarboxylates **19**, **25**, **28**, **31**, and **34**[a)]

Compd	Chemical shift[b)]									
	1	2	3	4	5	6	7	8	9	10
19	3.76 or 3.85 (CO_2Me)	2.36	2.03	2.69	3.05	1.48	3.76 or 3.85 (CO_2Me)	3.34	2.08	2.02
25	3.71 or 3.85 (CO_2Me)	3.02	2.04	2.71	2.79	1.32	3.54	3.43	3.71 or 3.85 (CO_2Me)	2.90
28	3.60	2.25	1.70	2.73	3.05	1.53	3.70 or 3.76 (CO_2Me)	3.60	3.70 or 3.76 (CO_2Me)	2.75
31	3.50	2.42	1.80	3.18	3.04	1.30	3.50	3.70 or 3.79 (CO_2Me)	3.70 or 3.79 (CO_2Me)	2.80
34[c)]	3.62	2.32	1.72	2.82	2.74	1.25	3.50	3.51	3.69 (CO_2Me)	2.47

Compd	Coupling constant J/Hz													
	1–2	1–3	1–9	1–10	2–4	3–4	4–5	4–6	4–8	5–7	6–7	7–8	8–9	8–10
19[d)]	—	—	—	—	9.5	0	8.6	0	6.4	—	—	—	3.9	0
25[e)]	—	—	—	—	9.6	0	8.3	0	5.6	7.6	0	7.3	—	0
28[f)]	6.1	0	—	0	9.2	0	8.6	0	5.6	—	—	—	—	0
31[g)]	6.6	0	—	0	8.6	0	8.4	0	—	8.4	0	—	—	0
34[h)]	6.3	0	—	0	8.5	0	8.2	0	—[i)]	—[i)]	0	—[i)]	—	0
Predicted Value[j)]	6.2	0.0	4.4	0.1	8.8	0.4	8.4	1.2	8.8	8.6	1.6	8.8	4.4	0.8

a) Spectra were determined with a JEOL JNM-GX-270 (270 MHz) in $CDCl_3$. b) Chemical shifts are shown in ppm (δ) relative to internal $SiMe_4$. Aromatic hydrogens of all compounds appeared at δ=6.9—7.2 (m, 3H for **34** and m, 4H for the other compounds). c) Another CO_2Me signal appeared at δ=3.89 (s, 3H). d) Geminal coupling constants are $J_{2-3}=13.2$, $J_{5-6}=11.6$, and $J_{9-10}=12.5$ Hz. e) Geminal coupling constants are $J_{2-3}=13.4$ and $J_{5-6}=11.2$ Hz and a long range coupling constant is $J_{4-7}=4.4$ Hz. f) Geminal coupling constants are $J_{2-3}=13.4$ and $J_{5-6}=11.3$ Hz. g) Geminal coupling constants are $J_{2-3}=13.2$ and $J_{5-6}=10.2$ Hz and a long range coupling constant is $J_{4-7}=4.5$ Hz. h) Geminal coupling constants are $J_{2-3}=13.2$ and $J_{5-6}=10.0$ Hz. i) Not determined due to the complexity of the signals. j) Calculated coupling constants on the basis of dihedral angles of 38.0, 81.6, 48.2, 74.4, 20.4, 98.9, 23.4, 105.7, 20.2, 21.8, 108.2, 20.2, 48.4, and 73.1 for 1–2, 1–3, 1–9, 1–10, 2–4, 3–4, 4–5, 4–6, 4–8, 5–7, 6–7, 7–8, 8–9, and 8–10, respectively, obtained from an optimized geometry for the mother compound by MM2 calculations.

between the observed attacking positions and the predicted positions from a spin-density consideration.

Factors Determining Position of Protonation. The observed positions of protonation are indicated in Chart 2 by arrows on the structural formulas of anions **17**, **20**, **21**, **26**, **29**, and **32**, the precursors of the reductive allylation products in the photoreactions of **2**—**6** with **7**. The results given in Chart 2 can be simplified, as shown in Chart 3, by deleting all substituents other than those directly attached to the anion part. Chart 3 indicates that protonation selectively occurs at the α-carbon atoms of the methoxycarbonyl groups. In anion **35** there are two α-carbon atoms of the methoxycarbonyl groups, and protonation occurs only at one of the α-carbon atoms, as shown in Chart 3.

Since the protonation of anions **17**, **20**, **21**, **26**, **29**, and **32** is thought to proceed under kinetically controlled conditions, the values of the net atomic charge at the allylic carbon atoms of the anions can essentially play an important role in determining the position of protonation. We thus carried out MNDO calculations[9)] on the net atomic charges of anions **33**—**35** with geometry optimization; the results are given in Table 5. These results show that the positions of protonation indicated by the arrows on the structural formulas of **33**—**35** in Chart 3 correspond well with those at which the highest negative charges occur among the carbon atoms of **33**—**35** in Table 5, and support the important role of the net negative charges of carbon atoms of the anions on determining the position of protonation.

Table 4. Spin Densities and Net Atomic Charges for the Radical Anions of Dimethyl Naphthalenedicarboxylates **2**—**6** by MNDO/RHF Calculations with Geometry Optimization

Radical Anion of Dimethyl 1,2-Naphthalenedicarboxylate (**2**)

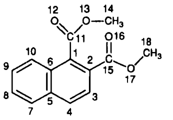

Atom number	Atom type	Spin density	Net atomic charge
1	C	0.2568	−0.2008
2	C	0.1328	−0.1265
3	C	0.0075	0.0288
4	C	0.1768	−0.1950
5	C	0.0194	0.0189
6	C	0.0001	0.0593
7	C	0.1020	−0.1252
8	C	0.0768	−0.1127
9	C	0.0326	−0.0615
10	C	0.1240	−0.1525
11	C	0.0033	0.4676
12	O	0.0041	−0.4042
13	O	0.0039	−0.3515
14	C	0.0016	0.2423
15	C	0.0276	0.4085
16	O	0.0258	−0.4187
17	O	0.0041	−0.3667
18	C	0.0001	0.2435

Radical Anion of Dimethyl 1,3-Naphthalenedicarboxylate (**3**)

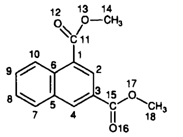

Atom number	Atom type	Spin density	Net atomic charge
1	C	0.1102	−0.2240
2	C	0.0022	0.1019
3	C	0.1266	−0.2327
4	C	0.2369	−0.0681
5	C	0.0222	−0.0124
6	C	0.0785	0.0145
7	C	0.1425	−0.1488
8	C	0.0036	−0.0379
9	C	0.1452	−0.1606
10	C	0.0615	−0.0796
11	C	0.0011	0.4516
12	O	0.0012	−0.4000
13	O	0.0016	−0.3502
14	C	0.0008	0.2355
15	C	0.0322	0.4254
16	O	0.0284	−0.4541
17	O	0.0047	−0.3600
18	C	0.0001	0.2453

Radical Anion of Dimethyl 1,4-Naphthalenedicarboxylate (**4**)

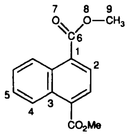

Atom number	Atom type	Spin density	Net atomic charge
1	C	0.2313	−0.2432
2	C	0.0859	0.0386
3	C	0.0064	0.0645
4	C	0.1094	−0.1437
5	C	0.0505	−0.0856
6	C	0.0054	0.4593
7	O	0.0047	−0.4069
8	O	0.0042	−0.3516
9	C	0.0021	0.2354

Radical Anion of Dimethyl 2,3-Naphthalenedicarboxylate (**5**)

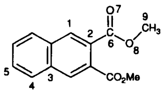

Atom number	Atom type	Spin density	Net atomic charge
1	C	0.2097	−0.1443
2	C	0.0514	0.0792
3	C	0.0005	0.0326
4	C	0.1616	−0.1734
5	C	0.0590	−0.0829
6	C	0.0086	0.4293
7	O	0.0016	−0.4015
8	O	0.0001	−0.3532
9	C	0.0001	0.2409

Radical Anion of Dimethyl 2,6-Naphthalenedicarboxylate (**6**)

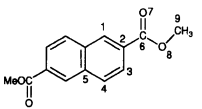

Atom number	Atom type	Spin density	Net atomic charge
1	C	0.1121	−0.0089
2	C	0.1644	−0.2422
3	C	0.0055	0.0254
4	C	0.0837	−0.1309
5	C	0.0762	−0.0477
6	C	0.0269	0.4301
7	O	0.0258	−0.4376
8	O	0.0046	−0.3649
9	C	0.0004	0.2431

Table 5. Net Atomic Charges for Anions **33**—**35** by MNDO Calculations with Geometry Optimization

Anion **33**

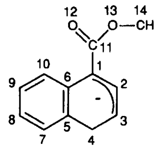

Atom number	Atom type	Net atomic charge
1	C	−0.4088
2	C	0.1002
3	C	−0.2928
4	C	0.1508
5	C	−0.1805
6	C	0.1619
7	C	−0.0103
8	C	−0.1889
9	C	−0.0305
10	C	−0.1522
11	C	0.4731
12	O	−0.4448
13	O	−0.3693
14	C	0.2443

Anion **34**

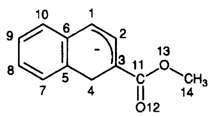

Atom number	Atom type	Net atomic charge
1	C	−0.3305
2	C	0.1548
3	C	−0.4230
4	C	0.1830
5	C	−0.1375
6	C	0.0990
7	C	−0.0256
8	C	−0.1600
9	C	−0.0475
10	C	−0.1354
11	C	0.4485
12	O	−0.4911
13	O	−0.3702
14	C	0.2508

Anion **35**

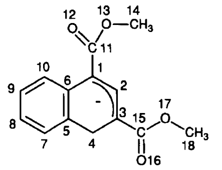

Atom number	Atom type	Net atomic charge
1	C	−0.3770
2	C	0.1988
3	C	−0.3915
4	C	0.1724
5	C	−0.1353
6	C	0.1288
7	C	−0.0276
8	C	−0.1476
9	C	−0.0456
10	C	−0.1253
11	C	0.4711
12	O	−0.4158
13	O	−0.3575
14	C	0.2380
15	C	0.4496
16	O	−0.4680
17	O	−0.3662
18	C	0.2472

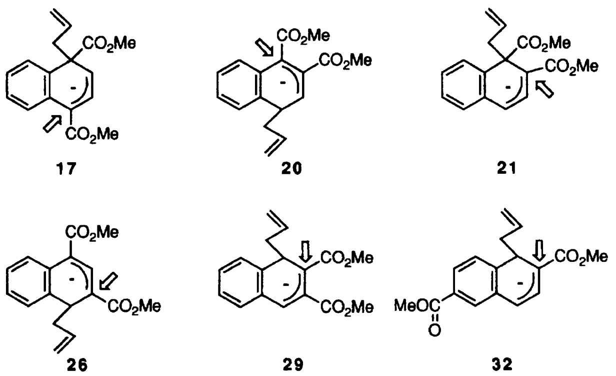

Chart 2.

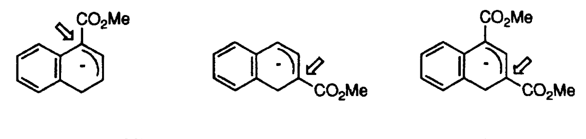

33 (model for **17**, **20**) **34** (model for **21**, **29**, **32**) **35** (model for **26**)

Chart 3.

The protonation of **33**—**35** to give reductive allylation products can proceed not only by direct protonation at the allylic carbon atoms, but also by a two-step mechanism, i.e., protonation at the carbonyl oxygen followed by enol–keto conversion. Table 5 indicates that the net negative charges of the carbonyl oxygen atoms of the methoxycarbonyl groups are somewhat higher than those of the corresponding α-carbon atoms of the methoxycarbonyl groups, and that in **35** the net negative charge of the carbonyl oxygen atom of atom number 16 in Table 5 is higher than that of the other carbonyl oxygen atom (atom number 12). Thus, the same prediction regarding the position of protonation can be obtained from both a consideration based on a direct protonation mechanism and from that based on a two-step mechanism.

Experimental

NMR spectra were obtained on a JEOL JNM-GX-270 (270 MHz) instrument. Chemical shifts are reported in ppm (δ) relative to internal $SiMe_4$. IR spectra were recorded by use of a Hitachi 260-50 spectrometer. Fluorescence spectra and fluorescence lifetimes were measured by a Hitachi 850 spectrophotometer and a Horiba NAES-1100 time-resolved spectrofluorimeter, respectively. Low-resolution (EI, 70 eV) and high-resolution (EI) mass spectra were measured on a Hitachi M-80B mass spectrometer. Melting points were recorded by using a Yanagimoto micro melting-point apparatus and are uncorrected. Combustion analyses were performed on a Yanagimoto CHN corder MT-5. The reduction potential was determined using a Yanaco cyclic polarography P-900. HPLC analyses were performed on a Hitachi 635S liquid chromatograph.

Materials. Methyl 2-naphthalenecarboxylate (**1**) was available from Tokyo Kasei Inc. and was used after recrystallization from ethanol. Dimethyl 1,2-naphthalenedicarboxylate (**2**), mp 84.0—85.0°C (from methanol, lit, 85°C)[10] was prepared by methyl esterification of 1,2-naphthalenedicarboxylic anhydride.[11] Dimethyl 1,3-naphthalenedicarboxylate (**3**), mp 102.5—104.0°C (from hexane–ether), ^{1}H NMR (CDCl$_3$) 4.01 (s, 3H), 4.03 (s, 3H), 7.5—7.8 (m, 4H), 7.99 (s, 1H), 8.02 (s, 1H), was prepared by methyl esterification of 1,3-naphthalenedicarboxylic acid.[10] Found: C, 68.74; H, 4.88%. Calcd for $C_{14}H_{12}O_4$: C, 68.84; H, 4.95%. Dimethyl 1,4-naphthalenedicarboxylate (**4**), mp 66.0—67.0°C (from hexane–ether, lit, 67°C)[10] was prepared by methyl esterification of 1,4-naphthalenedicarboxylic acid.[12] Dimethyl 2,3-naphthalenedicarboxylate (**5**), mp 45.0—46.0°C (from methanol, lit, 47°C)[10] was prepared by methyl esterification of commercially available 2,3-naphthalenedicarboxylic acid from Tokyo Kasei Inc. Dimethyl 2,6-naphthalenedicarboxylate (**6**) was obtained from Tokyo Kasei Inc. and was used after recrystallization from ethanol. Allyltrimethylsilane (**7**) was available from Shinetsu Chemicals Inc., and was purified by distillation. The solvents were purified by distillation after dehydration. Fluorescence-spectrograde acetonitrile, obtained from Nacalai Tesque Inc., was used as received for fluorescence spectrum measurements and lifetime determinations.

Fluorescence Quenching and Fluorescence Lifetime Measurements. For each quenching experiment five samples were prepared in 10 mL volumetric flasks, each containing 1.0×10^{-4} M of **1**—**6** and appropriate concentrations of **7** in acetonitrile. The fluorescence intensity at 358, 373, 367, 407, 362, and 377 nm was measured at 25°C for each sample at excitation wavelengths of 333, 295, 309, 317, 334, and 345 nm on the fluorescence quenching of **1**, **2**, **3**, **4**, **5**, and **6**, respectively. Stern–Volmer plots were linear; the slopes are given in Table 1. The fluorescence lifetimes were measured on air-saturated acetonitrile solutions containing 1.0×10^{-4} M of **1**—**6**.

General Procedure for Irradiation and Product Isolation. UV irradiation was carried out with an Eikosha EHB-WI-300 high-pressure Hg lamp with a uranium-filter (>320 nm) at ambient temperature. The reaction was monitored by TLC (Merck, Kieselgel 60 F$_{254}$) and by ^{1}H NMR measurements, and conducted to > 95% conversion. After evaporation of the solvent, the residue was subjected to column chromatography [Wakogel C-200 (silica gel, 74—149 μ; eluent, benzene–dichloromethane)] or HPLC (Wakopac-WS-5C8; eluent, methanol–water). The yields of the products based on the consumed **2**—**6** are given in the text.

Data for Photoproducts. Irradiation of 4 with 7. Data for Dimethyl (1*RS*,4*RS*)-1-Allyl-1,4-dihydronaphthalene-1,4-dicarboxylate (12): Oil; ^{1}H NMR (CDCl$_3$) δ=2.77 (dd, J=7.3, 13.9 Hz, 1H, 1H of CH$_2$), 2.90 (dd, J=6.8, 13.9 Hz, 1H, 1H of CH$_2$), 3.66 (s, 3H, CO$_2$Me), 3.71 (s, 3H, CO$_2$Me), 4.49 (dd, J=1.6, 4.2 Hz, 1H, C$\underline{\mathrm{H}}$CH=CH), 4.97 (d, J=10.0 Hz, 1H, 1H of =CH$_2$), 4.98 (d, J=17.1 Hz, 1H, 1H, of =CH$_2$), 5.63 (m, 1H, C$\underline{\mathrm{H}}$=CH$_2$), 5.96 (dd, J=1.6, 10.3 Hz, 1H, CHCH=C$\underline{\mathrm{H}}$), 6.12 (dd, J=4.2, 10.3 Hz, 1H, CHC$\underline{\mathrm{H}}$=CH), 7.2—7.4 (m, 4H, Arom H); IR (CHCl$_3$) 2945, 1736, 1436, 1228, 1196, 1158 cm^{-1}; MS m/z (rel intensity) 286 (M$^+$, 3), 245 (27), 227 (15), 213 (33), 201 (46), 169 (43), 155 (68), 142 (84), 127 (58); 115 (68), 59 (100), 57 (100), 43 (94), 41 (98). Found: m/z 286.1199. Calcd for $C_{17}H_{18}O_4$: M, 286.1204.

Data for Dimethyl (1*RS*,4*SR*)-1-Allyl-1,4-dihydronaphthalene-1,4-dicarboxylate (13): Oil; ^{1}H NMR (CDCl$_3$) δ=2.83 (dd, J=7.1, 14.1 Hz, 1H, 1H of CH$_2$), 2.90 (dd, J=6.8, 13.9 Hz, 1H, 1H of CH$_2$), 3.63 (s, 3H, CO$_2$Me), 3.69 (s, 3H, CO$_2$Me), 4.43 (dd, J=1.7, 4.3 Hz, 1H, C$\underline{\mathrm{H}}$CH=CH), 4.93 (dd, J=1.0, 10.0 Hz, 1H, 1H of =CH$_2$), 5.00 (dd, J=1.0, 17.0 Hz, 1H, 1H of =CH$_2$), 5.38 (m, 1H, C$\underline{\mathrm{H}}$=CH$_2$), 5.93 (dd, J=1.7, 10.2 Hz, 1H, CHCH=C$\underline{\mathrm{H}}$), 6.16 (dd, J=4.3, 10.2 Hz, 1H, CHC$\underline{\mathrm{H}}$=CH), 7.2—7.5 (m, 4H, Arom H); IR (CHCl$_3$) 2942, 1728, 1432, 1224, 1198, 1153 cm^{-1}; MS m/z (rel intensity) 286 (M$^+$, 6), 245 (33), 227 (22), 213 (46), 201 (49), 169 (46), 155 (77), 142 (82), 127 (68), 115 (57), 59 (100), 41 (98). Found: m/z 286.1182. Calcd for $C_{17}H_{18}O_4$: M, 286.1204.

Irradiation of 2 with 7. Data for Dimethyl (1*RS*,4*RS*)-4-Allyl-1,4-dihydronaphthalene-1,2-dicarboxylate (22): Oil; ^{1}H NMR (CDCl$_3$) δ=2.50 (ddd, J=7.0, 8.3, 13.2 Hz, 1H, 1H of CH$_2$), 2.56 (ddd, J=6.3, 7.0, 13.2 Hz, 1H, 1H of CH$_2$), 3.65 (m, 1H, C$\underline{\mathrm{H}}$CH$_2$), 3.69 (s, 3H, CO$_2$Me), 3.80 (s, 3H, CO$_2$Me), 4.78 (dd, J=1.3, 2.7 Hz, 1H, C$\underline{\mathrm{H}}$CO$_2$Me), 5.05 (d, J=17.5 Hz, 1H, 1H of =CH$_2$), 5.10 (d, J=9.5 Hz, 1H, 1H of =CH$_2$), 5.90 (m, 1H, C$\underline{\mathrm{H}}$=CH$_2$), 7.1—7.3 (m, 3H, Arom H), 7.40 (dd, J=1.3, 5.4 Hz, 1H, C$\underline{\mathrm{H}}$=CCO$_2$Me), 7.49 (d, J=7.1 Hz, 1H, Arom H); IR (CHCl$_3$) 2955, 1720, 1430, 1358, 1218 cm^{-1}; MS m/z (rel intensity) 286 (M$^+$, 3), 245 (6), 201 (8), 167 (11), 149 (52), 127 (12), 115 (18), 97 (19), 83 (24), 59 (100), 57 (88), 43 (96), 41 (93). Found: m/z 286.1208. Calcd for $C_{17}H_{18}O_4$: M, 286.1204.

Data for Dimethyl (1*RS*,4*SR*)-4-Allyl-1,4-dihydronaphthalene-1,2-dicarboxylate (23): Obtained as a mixture of **23** (80%) and **25** (20%); ^{1}H NMR (CDCl$_3$) δ= 2.58 (ddd, J=7.2, 7.6, 13.9 Hz, 1H, 1H of CH$_2$), 2.76 (ddd, J=4.3, 7.0, 13.9 Hz, 1H, 1H of CH$_2$), 3.60 (m, 1H, C$\underline{\mathrm{H}}$CH$_2$), 3.67 (s, 3H, CO$_2$Me), 3.80 (s, 3H, CO$_2$Me), 4.76 (d, J= 3.9 Hz, 1H, C$\underline{\mathrm{H}}$CO$_2$Me), 5.04 (d, J=10.0 Hz, 1H, 1H of =CH$_2$), 5.06 (d, J=16.9 Hz, 1H, 1H of =CH$_2$), 5.65 (m, 1H, C$\underline{\mathrm{H}}$=CH$_2$), 7.30 (d, J=3.9 Hz, 1H, C$\underline{\mathrm{H}}$=CCO$_2$Me), 7.0—7.5 (m, 4H, Arom H).

Data for Dimethyl (2*RS*,2a*SR*,3*SR*,4*RS*,8b*RS*)-1,2,2a,3,4,8b-Hexahydro-2,4-methanocyclobuta[*a*]naphthalene-3,4-dicarboxylate (25): Oil; ^{1}H NMR spectral data are shown in Table 3; IR (CHCl$_3$) 2955, 1736, 1432, 1258, 1198, 1173 cm^{-1}; MS m/z (rel intensity) 286 (M$^+$, 2), 245 (27), 213 (8), 201 (10), 187 (7), 167 (13), 142 (9), 127 (15), 115 (13), 59 (100), 41 (48). Found: m/z 286.1184. Calcd for $C_{17}H_{18}O_4$: M, 286.1204.

Irradiation of 3 with 7. Data for Dimethyl (2*RS*,2a*SR*,3*SR*,4*RS*,8b*RS*)-1,2,2a,3,4,8b-Hexahydro-2,4-methanocyclobuta[*a*]naphthalene-3,8b-dicarboxylate (28): Mp 91.0—92.0°C; ^{1}H NMR spectral data are shown in Table 3; ^{13}C NMR (CDCl$_3$) δ=33.15 (t), 38.16 (t), 38.68 (d), 47.24 (d), 50.98 (s), 51.53 (d), 51.78 (q), 52.03 (q), 125.28 (d), 126.43 (d), 126.60 (d), 127.25 (d), 138.25 (s), 144.47 (s), 173.42 (s) 174.83 (s); IR (CHCl$_3$) 2940, 1732, 1428, 1355, 1230, 1216, 1195 cm^{-1}; MS m/z (rel intensity) 286 (M$^+$, 7), 213 (8), 201 (18), 187 (11), 167 (21), 155 (18), 142 (23), 127 (16), 115 (13), 72 (33), 59 (100), 41 (56). Found: C, 71.26; H, 6.29%. Calcd for $C_{17}H_{18}O_4$: C, 71.31; H, 6.34%.

Irradiation of 5 with 7. Data for Dimethyl (2*RS*,2a*SR*,3*SR*,4*RS*,8b*RS*)-1,2,2a,3,4,8b-Hexahydro-2,4-methanocyclobuta[*a*]naphthalene-2a,3-dicarboxylate (31): Oil; ^{1}H NMR spectral data are shown in Table 3; IR (CHCl$_3$) 2950, 1735, 1435, 1252, 1204, 1178 cm^{-1}; MS m/z (rel intensity) 286 (M$^+$, 2), 226 (9), 213 (13), 201 (14), 186 (8), 167 (23), 149 (25), 127 (25), 115 (13), 73 (42), 59 (100), 43 (62), 41 (62). found: m/z 286.1216. Calcd for $C_{17}H_{18}O_4$: M, 286.1204.

Irradiation of 6 with 7. **Data for Dimethyl (2*RS*,2a*SR*,3*SR*,4*SR*,8b*RS*)-1,2,2a,3,4,8b-Hexahydro-2,4-methanocyclobuta[*a*]naphthalene-3,7-dicarboxylate (34):** Oil; ^{1}H NMR spectral data are shown in Table 3; ^{13}C NMR (CDCl$_3$) δ=35.88 (t), 37.14 (d), 38.91 (t), 39.56 (d), 41.75 (d), 47.59 (d), 51.64 (q), 51.85 (q), 52.32 (d), 126.09 (d), 126.90 (d), 128.45 (s), 128.63 (d), 141.64 (s), 150.36 (s), 166.99 (s), 173.74 (s); IR (CHCl$_3$) 2950, 1730, 1440, 1278, 1194, 1108, 1044 cm^{-1}; MS m/z (rel intensity) 286 (M$^+$, 3), 245 (38), 201 (25), 187 (45), 155 (40), 142 (54), 127 (37), 115 (17), 100 (19), 59 (100), 41 (62). Found: m/z 286.1194. Calcd for $C_{17}H_{18}O_4$: M, 286.1204.

Isomerization of 12 and 13 on Treatment with Base. To a solution of 45 mg of **12** in 10 mL of methanol was added 1 mL of ethanol solution of potassium hydroxide (125 mg in 10 mL of ethanol); the solution was left for 2 h at room temperature with stirring. The solution was then poured into 50 mL of water and extracted with chloroform. The extract was washed with water and dried over magnesium sulfate. After evaporation of the solvent, chromatography of the residue gave 40 mg (89%) of **18**. A similar treatment of 34 mg of **13** gave 27 mg (79%) of **18**.

Dimethyl (*RS*)-1-Allyl-1,2-dihydronaphthalene-1,4-dicarboxylate (18): Oil; ^{1}H NMR (CDCl$_3$) δ=2.50 (dd, J=4.8, 17.5 Hz, 1H, 1H of $C\underline{H}_2CH=$), 2.57 (dd, J=7.8, 14.2 Hz, 1H, 1H of $CH_2=CHC\underline{H}_2$), 2.79 (dd, J=7.8, 14.2 Hz, 1H, 1H of $CH_2=CHC\underline{H}_2$), 3.01 (dd, J=4.8, 17.5 Hz, 1H, 1H of $C\underline{H}_2CH=$), 3.69 (s, 3H, CO$_2$Me), 3.85 (s, 3H, CO$_2$Me), 5.08 (d, J=16.9 Hz, 1H, 1H of =CH$_2$), 5.10 (d, J=10.5 Hz, 1H, 1H of =CH$_2$), 5.74 (m, 1H, $CH_2C\underline{H}=CH_2$), 7.08 (t, J=4.8 Hz, 1H, $CH_2C\underline{H}=$), 7.2—7.4 (m, 4H, Arom H); IR (CHCl$_3$) 3040, 2960, 1735, 1442, 1262, 1038 cm^{-1}; MS m/z (rel intensity) 286 (M$^+$, 3), 245 (8), 227 (10), 213 (24), 167 (43), 149 (95), 128 (32), 127 (33), 115 (37), 59 (100), 57 (100), 55 (94), 41 (96). Found: m/z 286.1205. Calcd for $C_{17}H_{18}O_4$: M, 286.1204.

Irradiation of 18. Irradiation of an N$_2$-purged solution of 22 mg of **18** in 25 mL of acetonitrile gave **19** in almost quantitative yield.

Dimethyl (2*RS*,2a*RS*,4*SR*,8b*RS*)-1,2,2a,3,4,8b-Hexahydro-2,4-methanocyclobuta[*a*]naphthalene-4,8b-dicarboxylate (19): Mp 95.0—96.0°C; ^{1}H NMR spectral data are shown in Table 3; ^{13}C NMR (CDCl$_3$) δ=33.20 (t), 38.15 (t), 38.46 (t), 42.34 (d), 44.79 (d), 50.12 (s), 51.89 (q), 52.01 (q), 57.74 (s), 124.26 (d), 125.94 (d), 126.30 (d), 127.40 (d), 138.30 (s), 142.67 (s), 175.03 (s), 175.14 (s); IR (CHCl$_3$) 2945, 1734, 1430, 1282, 1232, 1214, 1138 cm^{-1}; MS m/z (rel intensity) 286 (M$^+$, 3), 245 (38), 213 (39), 201 (18), 187 (28), 167 (33), 155 (31), 142 (36), 127 (22), 115 (21), 72 (35), 59 (100), 41 (63). Found: C, 71.35; H, 6.38%. Calcd for $C_{17}H_{18}O_4$: C, 71.31; H, 6.34%.

Spin Density and Net Atomic Charge Calculations. Spin density and net atomic charge calculations were performed with MNDO Ver 2.0 in MOPAC (QCPE program No. 464) on IBM 3081-GX3 (Information Processing Center of Shimane University). All of the calculations were carried out by use of the key-word "precise"; the geometries were optimized starting from various starting structures.

This work was financially supported in part by a Grant-in-Aid for Scientific Research No. C-02640394 from the Ministry of Education, Science and Culture.

References

1) S. L. Mattes and S. Farid, *Org. Photochem.*, **6**, 233 (1983); M. Julliard and M. Channon, *Chem. Rev.*, **83**, 425 (1983); G. J. Kavarnos and N. J. Turro, *Chem. Rev.*, **86**, 401 (1986); J. J. McCullough, *Chem. Rev.*, **87**, 811 (1987); J. Mattay, *Angew. Chem., Int. Ed. Engl.*, **26**, 825 (1987); U. C. Yoon and P. S. Mariano, *Acc. Chem. Res.*, **25**, 233 (1992).

2) I. Saito, H. Ikehira, R. Kasatani, M. Watanabe, and T. Matsuura, *J. Am. Chem. Soc.*, **108**, 3115 (1986); J. Masnovi, *J. Am. Chem. Soc.*, **111**, 9081 (1989), and references cited therein.

3) a) K. Ohga and P. S. Mariano, *J. Am. Chem. Soc.*, **104**, 617 (1982); b) E. Hasegawa, M. A. Brumfield, and P. S. Mariano, *J. Org. Chem.*, **53**, 5435 (1988), and references cited therein.

4) a) K. Mizuno, M. Ikeda, and Y. Otsuji, *Tetrahedron Lett.*, **26**, 461 (1985); b) K. Mizuno, K. Terasaka, M. Ikeda, and Y. Otsuji, *Tetrahedron Lett.*, **26**, 5819 (1985); c) K. Mizuno, M. Ikeda, and Y. Otsuji, *Chem. Lett.*, **1988**, 1507; d) K. Mizuno, K. Nakanishi, and Y. Otsuji, *Chem. Lett.*, **1988**, 1833.

5) Y. Kubo, T. Imaoka, T. Shiragami, and T. Araki, *Chem. Lett.*, **1986**, 1749.

6) D. Rehm and A. Weller, *Isr. J. Chem.*, **8**, 259 (1970).

7) K. L. Williamson and W. S. Johnson, *J. Am. Chem. Soc.*, **83**, 4623 (1961).

8) S. Kyushin, Y. Ehara, Y. Nakadaira, and M. Ohashi, *J. Chem. Soc., Chem. Commun.*, **1989**, 279; S. Kyushin, Y. Nakadaira, and M. Ohashi, *Chem. Lett.*, **1990**, 2191; F. D. Saeva, D. T. Breslin, and H. R. Luss, *J. Am. Chem. Soc.*, **113**, 5333 (1991).

9) M. J. S. Dewar and W. Thiel, *J. Am. Chem. Soc.*, **99**, 4899 (1977).

10) E. F. Bradbrook and R. P. Linstead, *J. Chem. Soc.*, **1936**, 1739.

11) M. S. Newman, B. Dhawan, M. M. Hashem, V. K. Khanna, and J. M. Springer, *J. Org. Chem.*, **41**, 3925 (1976).

12) Z. Simon, A. T. Balaban, D. Ciubotariu, and T. S. Balaban, *Rev. Roum. Chim.*, **30**, 985 (1985).